Electromagnetic forces on the dielectric layers of the planar optical Bragg acceleration structure

Amit Mizrahi* and Levi Schächter
Department of Electrical Engineering, Technion—Israel Institute of Technology, Haifa 32000, Israel
(Received 12 May 2006; published 27 September 2006; publisher error corrected 28 September 2006)

Optical Bragg acceleration structures are waveguides with a vacuum core and dielectric layers as a cladding, designed to guide laser light at the speed-of-light TM mode and accelerate charged particles. In this study, we analyze the electromagnetic forces exerted on the dielectric layers of a planar structure by both the guided laser light and the wake-field of moving charges. The distribution of the volume force densities, as well as the surface force densities, in the interfaces between the layers as a result of the laser propagation is given, and analytic scaling laws for the maximal values are obtained. Separation of the wake-field into the structure's eigenmodes is essential in order to determine the different contributions of the wake-field to the total impulse that acts on the structure. It is shown that the impact of the wake-field on the structure results almost entirely from the fundamental TM mode. While the total force on the dielectric layers may be significantly stronger than the gravitational force, we show that for typical structures, the pressures that develop are orders of magnitude below the damage threshold.

DOI: 10.1103/PhysRevE.74.036504 PACS number(s): 29.17.+w, 41.75.Lx, 03.50.De, 78.70.−g

I. INTRODUCTION

Optical acceleration of charged particles, where particles are accelerated by laser light rather than by microwave radiation, is a subject of increasing interest. Due to the high loss of metals at optical wavelengths, optical acceleration structures are likely to be made of dielectric materials, which are also less susceptible to breakdown. One type of structure that may be used is an *open* optical structure, as in the LEAP [1] crossed laser beam experiment, where the interaction between the crossed laser beams and the particles is limited by slits to satisfy the Lawson-Woodward theorem [2,3]. Another type of structure is the dielectric waveguide, an example of which is the two-dimensional *photonic band-gap* structure with a vacuum tunnel bored in its center [4]. In such a configuration, a laser pulse propagates at the speed-of-light mode (phase velocity $v_{\mathrm{ph}}=c$) while accelerating a bunch of charged particles in the vacuum tunnel. Alternatively, one-dimensional photonic band-gap structures, namely, Bragg reflection waveguides [5–7] specifically designed for the speed-of-light mode, were suggested as acceleration structures [8]. A possible coupling scheme to this acceleration structure was recently proposed [9].

Optical Bragg acceleration structures, either planar or cylindrical, having typical transverse dimensions of a few microns, exhibit high performance as acceleration structures and therefore seem to be promising candidates for future optical accelerators. In the present study, we focus on the planar optical Bragg acceleration structure illustrated in Fig. 1. The laser light is guided between two mirrors separated by a distance $2D_{\mathrm{int}}$, so that the wave propagates along the z axis, and no variations are assumed along the y axis ($\partial/\partial y \equiv 0$). The mirrors consist of dielectric layers with alternating permittivity, having transverse quarter-wave width with the exception of the innermost layer. This first layer is a *matching layer* whose width is determined so that the structure supports the speed-of-light TM mode required for the acceleration process [8]. It was shown that, generally, Bragg waveguides may be designed for a given symmetric field distribution [10].

It is evident that if accelerators are to work at optical wavelengths, then the acceleration structures will be about three orders of magnitude smaller in the narrow transverse dimension of the cross section than current structures driven by microwave sources, as the structures will be made of micron-scale dielectrics instead of centimeter-size metallic walls. At the same time, the electromagnetic fields due to the traveling wave will be significantly stronger. Moreover, since the overall amount of charge is expected to remain similar to that of current accelerators, the electromagnetic wake-field resulting from the motion of these charges will be stronger as well. These intense electromagnetic fields exert forces on the dielectric structure, commonly referred to as "radiation pressure." Electromagnetic forces were previously investigated in photonic crystals [11], and the total pressure on the mirrors of Bragg reflection waveguides was demonstrated to be of great appeal subject to proper design [12,13]. It is the purpose of this study to evaluate these forces as they may impose constraints on future optical acceleration structures. Specifically, strong enough forces may deform the dielectric layers, change their width, and consequently detune the waveguide from the transverse resonance of the synchronized speed-of-light mode. Moreover, high pressures may cause crack formation and damage to the structure.

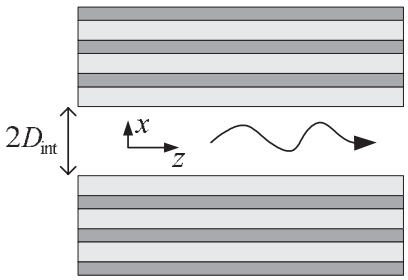

FIG. 1. Configuration of the planar optical Bragg accelerator.

*Electronic address: amitmiz@tx.technion.ac.il

The organization of this paper is as follows. In Sec. II, a general formulation of the Lorentz force densities in layered media is developed. In Sec. III, we examine the *time-averaged* forces exerted by laser light guided at the fundamental speed-of-light TM mode. A detailed analysis of the wake-field is given in Sec. IV, where the electromagnetic field excited by the moving charges is separated into the different modes of the structure. This crucial information is exploited in Sec. V for the evaluation of the impact of the wake-field on the optical Bragg acceleration structure.

II. GENERAL FORMULATION OF THE LORENTZ FORCE DENSITIES

In this section, we develop a general formulation of the force densities on dielectric layers in the presence of an electromagnetic field. The treatment here relies on macroscopic electromagnetic concepts, where the material is represented by a polarization density with associated polarization volume or surface currents and charges. The local Lorentz force may then be calculated directly, as resulting from the interaction of the electromagnetic field and these effective charges and currents [14]. In a similar approach, Planck [15] calculated the pressure exerted by a plane wave incident upon a metallic plate. In addition to the expressions for a general electromagnetic field, we are interested in the time-averaged expressions of a time-harmonic signal. Recently, this approach was used for the calculation of optical forces [16].

A. Volume force densities

Within the dielectric layers, the Lorentz volume force density is given by

$$\vec{f} = \rho\vec{\mathcal{E}} + \vec{\mathcal{J}} \times \vec{\mathcal{B}}, \tag{1}$$

where ρ is the instantaneous electric charge density, $\vec{\mathcal{J}}$ is the instantaneous electric current density, $\vec{\mathcal{E}}$ is the instantaneous electric field, and $\vec{\mathcal{B}}$ is the instantaneous magnetic induction. In a polarizable material with instantaneous polarization density $\vec{\mathcal{P}}$, the macroscopic effective charge density is $\rho = -\nabla \cdot \vec{\mathcal{P}}$, and the effective current density is $\vec{\mathcal{J}} = \partial\vec{\mathcal{P}}/\partial t$. Since in a dielectric material $\varepsilon_0\varepsilon_r\vec{\mathcal{E}} = \varepsilon_0\vec{\mathcal{E}} + \vec{\mathcal{P}}$ and $\nabla \cdot \vec{\mathcal{E}} = 0$ as there is no free charge, it follows that $\rho = 0$. Therefore only the second term in Eq. (1) is nonzero, and the volume force density, using $\vec{\mathcal{B}} = \mu_0\vec{\mathcal{H}}$, reads

$$\vec{f} = \varepsilon_0(\varepsilon_r - 1)\frac{\partial\vec{\mathcal{E}}}{\partial t} \times \mu_0\vec{\mathcal{H}}. \tag{2}$$

Specifically, for time harmonic fields of time-dependence $e^{j\omega t}$, the time-average force density is given by

$$\langle\vec{f}\rangle = \frac{1}{2}\,\mathrm{Re}[-j\omega\varepsilon_0(\varepsilon_r - 1)\vec{E}^* \times \mu_0\vec{H}], \tag{3}$$

where $\vec{E}$ and $\vec{H}$ are the frequency domain electric and magnetic fields, respectively.

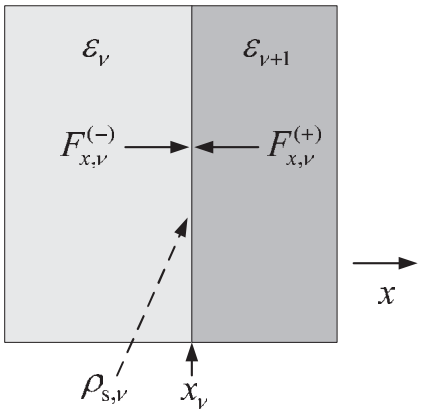

FIG. 2. An interface between two dielectric layers, where a polarization surface charge density is formed.

B. Surface force densities

At the interfaces between the dielectric layers, a polarization surface charge is created, giving rise to a surface force density. The instantaneous polarization surface charge between layer ν and layer $\nu+1$, as shown in Fig. 2, is given by

$$\rho_{s,\nu} = -\vec{1}_x \cdot (\vec{\mathcal{P}}^{(-)}_{\nu+1} - \vec{\mathcal{P}}^{(+)}_{\nu}), \tag{4}$$

where $\vec{\mathcal{P}}^{(-)}_{\nu+1}$ and $\vec{\mathcal{P}}^{(+)}_{\nu}$ are the polarization densities at the interface in layer $\nu+1$ and layer ν, respectively. The Lorentz force per unit area is obtained by multiplying the polarization surface charge density by the *average* of the perpendicular electric fields from both sides of the discontinuity [15]. Defining $\mathcal{E}^{(+)}_{x,\nu}$ and $\mathcal{E}^{(-)}_{x,\nu+1}$ as the x components of the electric field at the boundary in layer ν and layer $\nu+1$, respectively, we obtain for the surface force density

$$F_{x,\nu} = \rho_{s,\nu}\frac{1}{2}(\mathcal{E}^{(+)}_{x,\nu} + \mathcal{E}^{(-)}_{x,\nu+1}). \tag{5}$$

Using the boundary condition $\varepsilon_\nu\mathcal{E}^{(+)}_{x,\nu} = \varepsilon_{\nu+1}\mathcal{E}^{(-)}_{x,\nu+1}$ together with Eq. (4), the surface force density at the boundary reads

$$F_{x,\nu} = \frac{1}{2}\varepsilon_0(\mathcal{E}^{(+)}_{x,\nu})^2\left(\frac{\varepsilon^2_\nu}{\varepsilon^2_{\nu+1}} - 1\right). \tag{6}$$

This total surface force density may be conveniently divided into two contributions from the two polarization densities of each layer at the interface. For this purpose, we may postulate the existence of an infinitesimal vacuum gap between the two layers, and then the force density is calculated on each of the two surface polarization charges. The force density on the surface charge of layer ν is given by

$$F^{(-)}_{x,\nu} = \frac{1}{2}\varepsilon_0(\mathcal{E}^{(+)}_{x,\nu})^2(\varepsilon^2_\nu - 1) > 0, \tag{7}$$

and the force density on the polarization surface charge of layer $\nu+1$ is

$$F_{x,\nu}^{(+)} = -\frac{1}{2}\varepsilon_0(\mathcal{E}_{x,\nu+1}^{(+)})^2(\varepsilon_{\nu+1}^2 - 1) < 0, \tag{8}$$

and $F_{x,\nu}=F_{x,\nu}^{(-)}+F_{x,\nu}^{(+)}$. In the two above inequalities, we have assumed that $\varepsilon_\nu > 1$, leading to the conclusion that the effect of these forces is to pull each of the two layers at the interface towards the other, as illustrated in Fig. 2. For time-harmonic fields, the time-average of the surface force densities is readily obtained by multiplying the expressions of Eqs. (6)–(8) by 1/2 and replacing the time-dependent electric fields by the absolute value of the complex fields.

III. FUNDAMENTAL MODE FORCES

Let us consider a planar acceleration structure guiding laser light at wavelength λ_0 with corresponding angular frequency $\omega_0=2\pi c/\lambda_0$. In what follows we shall examine the time-averaged force densities on the structure. In the vacuum core, the speed-of-light TM mode guided by the structure, assuming a time dependence of $e^{j\omega_0 t}$, is of the form [8]

$$E_z = E_0 e^{-j(\omega_0/c)z},$$

$$E_x = E_0\left(j\frac{\omega_0}{c}x\right)e^{-j(\omega_0/c)z},$$

$$H_y = \frac{E_0}{\eta_0}\left(j\frac{\omega_0}{c}x\right)e^{-j(\omega_0/c)z}. \tag{9}$$

The total transverse pressure exerted on the mirrors may be found by integrating the time-averaged Maxwell stress-tensor [17] over a closed surface. Within the vacuum core, the time-averaged Maxwell stress-tensor component $\langle T_{xx}\rangle$ for a TM mode reads

$$\langle T_{xx}\rangle = \frac{1}{4}\varepsilon_0|E_x|^2 - \frac{1}{4}\varepsilon_0|E_z|^2 - \frac{1}{4}\mu_0|H_y|^2, \tag{10}$$

and given Eq. (9), we are left with

$$\langle T_{xx}\rangle = -\frac{1}{4}\varepsilon_0|E_0|^2. \tag{11}$$

Enclosing one mirror by a rectangular surface, only the T_{xx} component contributes to the integral, as the T_{xz} component has zero contribution due to symmetry, and the T_{xy} component is identically zero. Assuming that the laser field decays to zero at $x=\pm\infty$, the time-averaged transverse pressure exerted by the guided mode on the Bragg mirror located at $x=D_{\text{int}}$ is

$$\langle F_{x,\mathrm{T}}\rangle = \frac{1}{4}\varepsilon_0|E_0|^2; \tag{12}$$

the subscript T indicates total pressure. Hence, for a given accelerating gradient E_0, the total transverse pressure is repelling and is independent of the details of the structure, that could be, for example, a dielectric loaded metallic transmission line. For comparison purposes, we note that this pressure is 1/4 of the pressure exerted by a plane wave of amplitude E_0 incident *perpendicularly* upon a perfect metallic plate. Assuming that the gradient of interest is $E_0=1$ GV/m, the total pressure is $\langle F_{x,\mathrm{T}}\rangle \simeq 2.2\times10^{-6}$ N/μm^2.

Evaluation of the time-averaged volume force densities of the acceleration TM mode is performed next according to Eq. (3). The transverse component is given by

$$\langle f_x\rangle = \frac{1}{2}\,\mathrm{Re}[j\omega_0\varepsilon_0(\varepsilon_r - 1)E_z^*\mu_0 H_y]. \tag{13}$$

Bearing in mind that the ratio H_y/E_x inside the lossless dielectric layers is a real constant, the longitudinal component of the volume force density reads

$$\langle f_z\rangle = \frac{1}{2}\,\mathrm{Re}[-j\omega_0\varepsilon_0(\varepsilon_r - 1)E_x^*\mu_0 H_y] = 0, \tag{14}$$

which vanishes as it is the real part of an imaginary quantity. The third component of the volume force density is $f_y \equiv 0$ for TM modes. The surface force densities are computed using the time-average of Eqs. (6)–(8), so that the total pressure, given by Eq. (12), is the sum of all transverse force densities, and explicitly,

$$\langle F_{x,\mathrm{T}}\rangle = \sum_{\nu=0}^{\infty}\left[\langle F_{x,\nu}\rangle + \int_{x_\nu}^{x_{\nu+1}} dx\langle f_x(x)\rangle\right]; \tag{15}$$

x_ν denotes the boundary between layer ν and layer $\nu+1$ (see Fig. 2), and $\nu=0$ denotes the core. Practically, the above equation may be verified numerically by carrying out the summation up to some layer where the fields have sufficiently decayed to be considered negligible.

The above expressions for the force densities may now be utilized for Bragg acceleration structures, and particularly, the analysis of two structures made of SiO_2 ($\sqrt{\varepsilon_r}=1.45$) and Si ($\sqrt{\varepsilon_r}=3.45$) with core half-width $D_{\text{int}}=0.3\lambda_0$ is given in Fig. 3 (volume force densities) and Fig. 4 (surface force densities). In each figure, the frames in the left column correspond to a structure having the SiO_2 as the matching layer adjacent to the core, and the right column corresponds to a structure with Si as the layer adjacent to the core. When the lower refractive index is used for the matching layer, the maximum of the volume force density is obtained inside the second layer [Fig. 3(c)], whereas in the second case, the maximum is obtained inside the matching layer [Fig. 3(d)]. The surface force densities $\langle F_{x,\nu}^{(-)}\rangle$, $\langle F_{x,\nu}^{(+)}\rangle$, and $\langle F_{x,\nu}\rangle$, are shown in Fig. 4. The total surface force density $\langle F_{x,\nu}\rangle$ [Figs. 4(e) and 4(f)] peaks at the vacuum-dielectric interface. Inside the periodic part of the Bragg mirror, E_x vanishes every other interface [8], and accordingly, all three surface force densities vanish as well.

The total internal pressure at some point within the layers against an external mechanical enforcement is given by the cumulative sum of both surface and volume force densities starting from the vacuum core up to the point of interest, similarly to the sum of Eq. (15), which is up to $x=\infty$. This pressure, which we denote by $\langle F_{\text{pr}}\rangle$, is depicted in Figs. 3(e) and 3(f). It is seen that in the layers that are close to the vacuum core, the pressure is negative, pulling these layers towards the core. Farther away from the core, the pressure

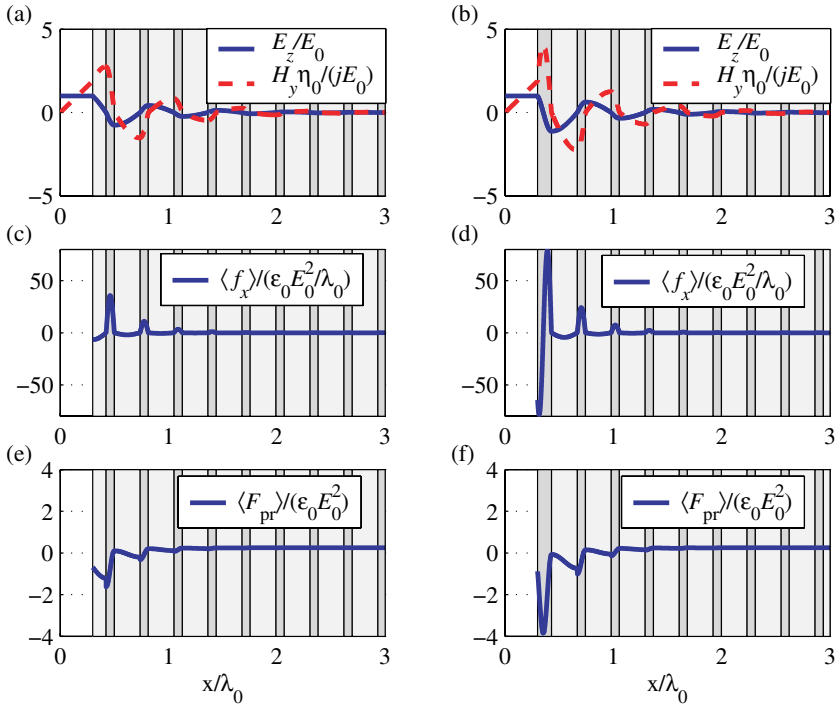

FIG. 3. (Color online). Volume force densities in two Bragg structures made of SiO_2 (indicated by lighter gray) and Si. (a) and (b) Two of the electromagnetic field components, (c) and (d) volume force densities, and (e) and (f) total internal pressure. The left column frames correspond to a structure with SiO_2 as the matching layer, and the right column corresponds to Si as the matching layer.

becomes positive and approaches $\langle F_{x,T}\rangle = \frac{1}{4}\varepsilon_0|E_0|^2$ (not seen clearly in the figure due to the scale).

It is worth noting that for the structure with SiO_2 as the matching layer, as can be seen in Fig. 3(a), E_z vanishes at the interface of the matching layer and the bordering layer, and therefore, the electromagnetic field of this structure up to the plane $x=x_1$ is identical to that of a dielectric loaded transmission line. Obviously, the electromagnetic forces exerted on the dielectric layers inside the transmission line would be identical to the forces shown here on the matching layer in Figs. 3(c) and 3(e), and Figs. 4(a), 4(c), and 4(e).

Assuming that the accelerating gradient E_0 remains constant, the larger the core half-width D_{int} is, the stronger the fields at the vacuum-dielectric interface are, and consequently, the forces inside the dielectric layers become stronger. In Fig. 5 we consider acceleration structures with SiO_2 as the matching layer and with D_{int} ranging from $0.3\lambda_0$ to $0.8\lambda_0$ and plot the maximal values of the force densities, $|\langle f_x\rangle|_{max}$, $|\langle F_x\rangle|_{max}$, $|\langle F_x^{(+)}\rangle|_{max}$, and $|\langle F_x^{(-)}\rangle|_{max}$, in each device. For each value of D_{int}, the device is designed according to the principles given in Ref. [8], so that the $k_z=\omega_0/c$ acceleration mode is supported by the structure. By calculating

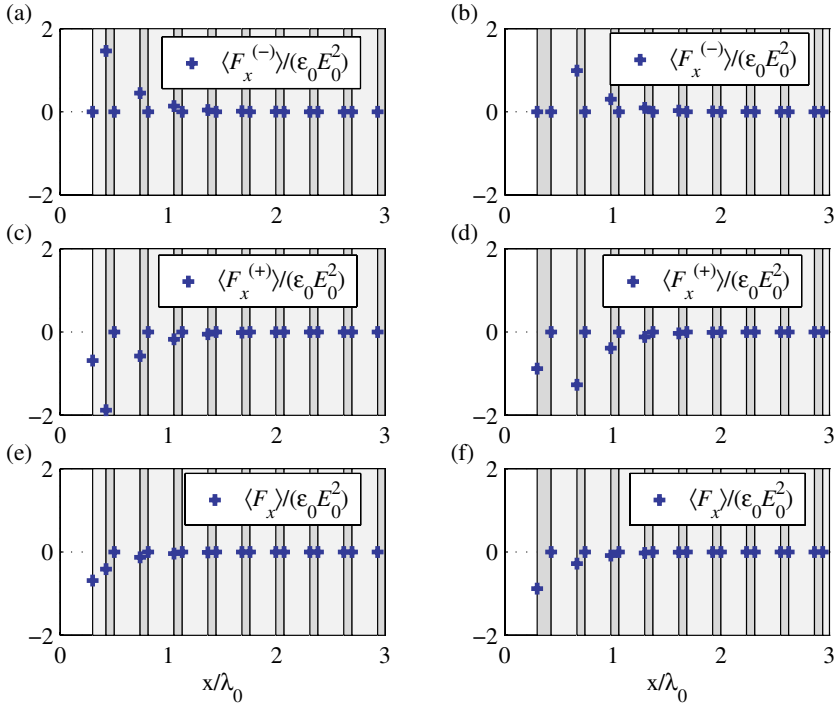

FIG. 4. (Color online). Surface force densities in two Bragg structures made of SiO_2 (indicated by lighter gray) and Si. (a) and (b) Left sided force $\langle F_{x,\nu}^{(-)}\rangle$, (c) and (d) right sided force $\langle F_{x,\nu}^{(+)}\rangle$, and (e) and (f) total force $\langle F_{x,\nu}\rangle$. The left column frames correspond to a structure with SiO_2 as the matching layer, and the right column corresponds to Si as the matching layer.

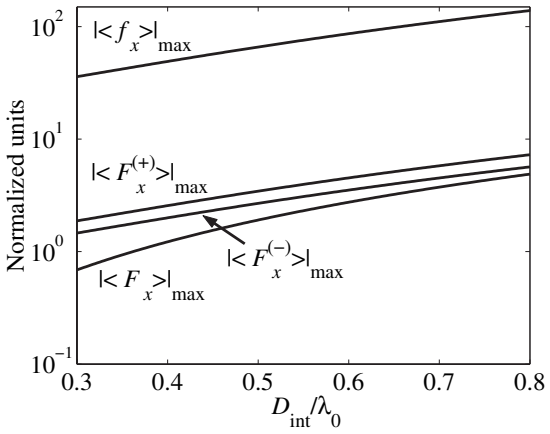

FIG. 5. Maximal values of the volume and surface force densities as a function of the core half-width for a structure having SiO_2 as the matching layer. The maximal volume force density $|\langle f_x\rangle|_{max}$ is normalized by $\varepsilon_0 E_0^2/\lambda_0$, whereas the surface force densities are normalized by $\varepsilon_0 E_0^2$.

the fields inside the dielectric layers given the vacuum field [Eq. (9)], it is possible to show that the behavior of the maximal volume force density takes the form

$$|\langle f_x\rangle|_{max} = \kappa\frac{\pi}{2}\left[1+\left(\frac{\omega_0 D_{int}}{c}\right)^2\frac{\varepsilon_1-1}{\varepsilon_1^2}\right]\frac{\varepsilon_0|E_0|^2}{\lambda_0}, \quad (16)$$

where κ is a constant independent of D_{int}. When the maximum is obtained in the matching layer, $\kappa=\varepsilon_1\sqrt{\varepsilon_1-1}$, and when the maximum is in the second layer, as in the case of Fig. 5, $\kappa=(\varepsilon_2-1)Z_2/Z_1^2$, where $Z_\nu=\eta_0\sqrt{\varepsilon_\nu-1}/\varepsilon_\nu$, $\nu=1,2$ are the transverse impedances. Since the maximal surface force density is obtained at the vacuum-dielectric interface, Eq. (6) may be used to calculate directly this quantity, which is given by

$$|\langle F_x\rangle|_{max} = \frac{1}{4}\left(\frac{\omega_0 D_{int}}{c}\right)^2\frac{\varepsilon_1^2-1}{\varepsilon_1^2}\varepsilon_0|E_0|^2. \quad (17)$$

The two above equations are scaling laws that are among the main results of this study.

IV. WAKE-FIELD ANALYSIS

A general treatment of wake-fields in dielectric acceleration structures was given in Ref. [18], and the wake-field of a line-charge inside a Bragg structure was considered in Ref. [8]. In this section, we further investigate the wake-field in a Bragg acceleration structure, separating the wake into the structure's eigenmodes following a method proposed in Ref. [8]. This analysis is utilized in the subsequent section for the evaluation of the impact of the wake-field on the acceleration structure.

A. The general wake-field integral

We are interested in the wake-field created by a line-charge, infinite in the y direction, and moving in the z direction within the acceleration structure with a constant velocity v, or explicitly, having the current density

$$\mathcal{J}_z(x,z,t) = -qv\delta(x)\delta(z-vt), \quad (18)$$

where $(-q)$ is the charge per unit length. The electromagnetic field in the vacuum core is divided into two contributions: the field generated by the line-charge in free space (primary field), and the field reflected from the surrounding structure (secondary field). In the ultrarelativistic limit $[\gamma=(1-v^2/c^2)^{-1/2}\to\infty]$, the secondary longitudinal electric field is given by [8]

$$\mathcal{E}_z^{(sec)}(\tau) = \frac{E_q}{2}\int_{-\infty}^{\infty} d\bar{\omega}e^{j\bar{\omega}\bar{\tau}}\frac{1}{\frac{1-\mathbb{R}(\bar{\omega})}{1+\mathbb{R}(\bar{\omega})}+j\bar{\omega}}. \quad (19)$$

In the above equation, $E_q \triangleq q/(2\pi\varepsilon_0 D_{int})$, $\tau \triangleq t-z/c$, $\xi \triangleq \sqrt{\varepsilon_1-1}D_{int}/(\varepsilon_1 c)$, $\bar{\omega}\triangleq\xi\omega$, $\bar{\tau}\triangleq\tau/\xi$, and ε_1 is the dielectric coefficient of the material adjacent to the vacuum region. The surrounding structure is represented by the reflection coefficient $\mathbb{R}(\bar{\omega})$, which is the relation between the outgoing and incoming waves just outside the vacuum tunnel. Thus the wake-field is given as a spectrum of propagating waves, all having longitudinal wave number $k_z=\omega/c$.

B. Wake-field initial and final values

As will be shown in the subsequent section, the value of the deceleration force on the moving particle is essential for the understanding of the separation of the wake to the structure's eigenmodes. It was previously pointed out in Refs. [8,18] that in case of a single particle, this deceleration force is dependent only on the size of the vacuum core and the permittivity of the material surrounding the structure, rather than on the details of the structure at $x>D_{int}$. We shall next present a general proof of this concept, based on the initial value theorem [19].

Due to causality, $\mathcal{E}_z^{(sec)}(\tau<0)=0$, and therefore the inverse Fourier transform of Eq. (19) obeys the initial value theorem, which states that

$$\mathcal{E}_z^{(sec)}(0^+) = \lim_{\bar{\omega}\to\infty} j\bar{\omega}2\pi\frac{E_q/2}{\frac{1-\mathbb{R}(\bar{\omega})}{1+\mathbb{R}(\bar{\omega})}+j\bar{\omega}}$$

$$= \lim_{\bar{\omega}\to\infty}\frac{\pi E_q}{1+\frac{1}{j\bar{\omega}}\frac{1-\mathbb{R}(\bar{\omega})}{1+\mathbb{R}(\bar{\omega})}}. \quad (20)$$

If we consider any practical structure, then the reflection coefficient satisfies $|\mathbb{R}(\bar{\omega})|<1$, and therefore $|[1-\mathbb{R}(\bar{\omega})]/[1+\mathbb{R}(\bar{\omega})]|$ is both upper and lower bounded, and Eq. (20) becomes

$$\mathcal{E}_z^{(sec)}(0^+) = \pi E_q. \quad (21)$$

The decelerating field is the secondary field acting on the charged particle at its own location, which is the average of the inverse Fourier transform values at $\mathcal{E}_z^{(sec)}(0^+)$ and $\mathcal{E}_z^{(sec)}(0^-)$, given by

$$\mathcal{E}_{\text{dec}} = \frac{\pi}{2} E_q = \frac{\pi}{2} \frac{q}{2\pi\varepsilon_0 D_{\text{int}}}. \tag{22}$$

For completeness, we may also employ the final value theorem [19] to obtain the value of the wake-field at $\tau \to \infty$, which reads

$$\lim_{\tau\to\infty} \mathcal{E}_z^{(\text{sec})}(\tau) = \lim_{\bar{\omega}\to 0} j\bar{\omega} 2\pi \frac{E_q/2}{\frac{1-\mathbb{R}(\bar{\omega})}{1+\mathbb{R}(\bar{\omega})} + j\bar{\omega}} = 0. \tag{23}$$

Clearly, the wake-field decays to zero a sufficiently long time after the charge passes, since the electromagnetic field that follows it escapes from the structure. The conclusions drawn here apply also for a closed structure, such as the dielectric loaded transmission line, if it is conceived as having infinitesimal losses.

C. Wake-field and eigenmodes

The denominator in the integrand of Eq. (19) is, in fact, the dispersion function for $k_z = \omega/c$, such that zeros of this function (poles of the integrand) are eigenfrequencies of the structure. Thus the dispersion function $F(\bar{\omega})$ is defined over the complex $\bar{\omega}$ plane by

$$F(\bar{\omega}) \triangleq \frac{1-\mathbb{R}(\bar{\omega})}{1+\mathbb{R}(\bar{\omega})} + j\bar{\omega}. \tag{24}$$

Although it is possible to perform the integral of Eq. (19) numerically, when the structure is more confining, the integrand becomes closer to being singular, making the integration a more difficult numerical task. Specifically for the Bragg structure, when more layers are added, the structure guides the propagating modes with less confinement losses, and the poles are closer to the real $\bar{\omega}$ axis. Another possibility for evaluation of the wake-field integral, as suggested in Ref. [8], is to use the residue theorem, resulting in the expression

$$\mathcal{E}_z^{(\text{sec})}(\tau) = \frac{E_q}{2} \sum_n 2\pi j \frac{1}{F'(\bar{\omega}_n)} e^{j\bar{\omega}_n \bar{\tau}} u(\tau), \tag{25}$$

where the prime denotes derivative with respect to $\bar{\omega}$, $\bar{\omega}_n$ are the zeros of $F(\bar{\omega})$, and $u(\tau)$ is the unit step function defined by

$$u(\tau) \triangleq \begin{cases} 0, & \tau < 0 \\ 0.5, & \tau = 0 \\ 1, & \tau > 0. \end{cases} \tag{26}$$

Except for a zero that may be on the imaginary $\bar{\omega}$ axis, all the zeros appear in complex conjugate pairs. It is, therefore, possible to rewrite Eq. (25) as a summation over zeros with non-negative real part only, in the form

$$\mathcal{E}_z^{(\text{sec})}(\tau) = \pi E_q \sum_{n=1}^{\infty} W_n \cos(\omega_{\text{R},n}\tau + \psi_n) e^{-\omega_{\text{I},n}\tau} u(\tau), \tag{27}$$

where the weights W_n are real and positive, ψ_n are real, $\omega_n = \bar{\omega}_n/\xi \triangleq \omega_{\text{R},n} + j\omega_{\text{I},n}$, and according to Eq. (21), we obtain

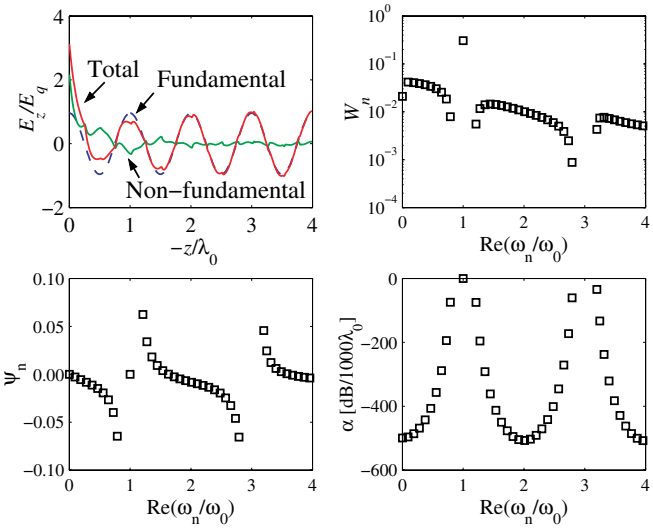

FIG. 6. (Color online). Wake-field in a SiO_2-Si structure with $D_{\text{int}} = 0.3\lambda_0$. Top left: The longitudinal electric field at $t=0$ divided into the fundamental, nonfundamental, and total contributions. Top right: the mode weights W_n. Bottom left: the mode phases ψ_n. Bottom right: the mode attenuation α per $1000\lambda_0$.

$$\sum_{n=1}^{\infty} W_n \cos(\psi_n) = 1. \tag{28}$$

Two extreme cases of planar structures that are relevant to the present discussion are the dielectric loaded metallic (or perfect magnetic) transmission line, and a vacuum tunnel bored in a homogeneous dielectric material. In the first case, the closed structure has truly guided eigenmodes at real frequencies $\bar{\omega}_n$. The second exhibits only one zero of the dispersion function $F(\bar{\omega})$ on the imaginary axis of the complex $\bar{\omega}$ plane, corresponding to a pure exponential decay. The Bragg structure is in between the two aforementioned cases, having modes with both oscillations and exponential decay, including one zero on the imaginary axis. The decay of the modes is due to both the confinement losses caused by the finite number of Bragg layers, and to the passbands allowing waves to propagate transversally, and thus escape the structure. For the Bragg structure, an analytic expression exists for the reflection coefficient $\mathbb{R}(\bar{\omega})$, and therefore, both $F(\bar{\omega})$ and $F'(\bar{\omega})$ have an analytic expression as well. However, the zeros in the complex plane of $F(\bar{\omega})$ are found numerically.

As a reasonable configuration, we consider a Bragg structure with $D_{\text{int}} = 0.3\lambda_0$, having a matching layer made of SiO_2 and ten periods of alternating Si and SiO_2 transverse quarter-wave layers $[\lambda_0/(4\sqrt{\varepsilon_\nu - 1})]$. In Fig. 6 (top left), the total longitudinal electric field is presented, as well as the fundamental mode only, and a curve representing the remainder of the modes. After only a few fundamental mode wavelengths behind the charge, the nonfundamental modes undergo considerable attenuation, and the fundamental mode is the dominant part of the wake. The weights W_n and the relative phases ψ_n of Eq. (27) are presented in the top right and the bottom left frames of Fig. 6, respectively, as a function of $\omega_{\text{R},n}$. There are about ten modes per ω_0 corresponding to the ten periods of the transverse periodic structure. As can be

seen, the dominant weight, W_{11}, is that of the fundamental mode at $\omega_{R,11}=\omega_0$ with $\psi_{11}\cong 0$. We shall denote the weight of the fundamental mode by W_{fun}, and here $W_{\mathrm{fun}}\cong 0.305$, which means that it is responsible for about 30% of the deceleration force acting on the moving charge. The weight of the fundamental mode may also be calculated from the cold parameters of the structure by [20,21]

$$W_{\mathrm{fun}} \cong \frac{Z_{\mathrm{int}}}{\eta_0 \lambda_0}\frac{D_{\mathrm{int}}}{\lambda_0}\frac{\beta_{\mathrm{gr}}}{1-\beta_{\mathrm{gr}}}, \tag{29}$$

where the interaction impedance is given by $Z_{\mathrm{int}}=|\lambda_0 E_0|^2/P$, P being the flowing power per unit length in y, and $\beta_{\mathrm{gr}}=v_{\mathrm{gr}}/c$ is the normalized group velocity. The longitudinal attenuation per $1000\lambda_0$ of each one of the modes that form the wake-field is given in Fig. 6 (bottom right), calculated directly from $\omega_{\mathrm{I},n}$. The fundamental mode has an attenuation of 0.13 dB/$1000\lambda_0$, and there are 15 more modes below $100\omega_0$ that have an attenuation of less than 3 dB/$1000\lambda_0$ and may therefore be considered guided modes.

V. WAKE-FIELD EFFECT ON THE STRUCTURE

The wake-field analysis in the previous section is used in this section for the evaluation of the wake's impact on the structure. Since the wake-field is a transient phenomena, the quantity of interest is the impulse that acts on the structure. The related problem of momentum transfer from passing electrons to small particles was previously addressed [22]. Subsequently to the evaluation of the impact of the wake-field alone, we estimate the combined effect of the wake and the driving laser.

A. The impulse integral

In order to evaluate the wake-field impulse, we enclose a section of the top Bragg mirror of Fig. 1 by a rectangular box having length Δ_z and width Δ_y, and the bottom of the box is at some $0<x_{\mathrm{in}}<D_{\mathrm{int}}$. It is assumed that beyond the outermost dielectric layer, there is a layer of material that absorbs the Cerenkov radiation emitted by the charges, located at x_{out}. That is to say that the structure absorbs all of the emitted radiation. The total force $\mathcal{F}_x(t)$ may be written in terms of the Maxwell stress-tensor components $T_{xx}(x,z,t)$ and $T_{xz}(x,z,t)$, bearing in mind that $T_{xy}\equiv 0$, by

$$\mathcal{F}_x(t) = \Delta_y \int_0^{\Delta_z} dz[-T_{xx}(x_{\mathrm{in}},z,t)] + \Delta_y \int_{x_{\mathrm{in}}}^{x_{\mathrm{out}}} dx[-T_{xz}(x,0,t)] + \Delta_y \int_{x_{\mathrm{in}}}^{x_{\mathrm{out}}} dx T_{xz}(x,\Delta_z,t) - \frac{1}{c^2}\frac{d}{dt}\Delta_y \int_0^{\Delta_z} dz \int_{x_{\mathrm{in}}}^{x_{\mathrm{out}}} dx(\vec{\mathcal{E}} \times \vec{\mathcal{H}}) \cdot \vec{1}_x. \tag{30}$$

For the total impulse, the instantaneous force is integrated in time. After the integration, the second and third terms of the right-hand side of Eq. (30) cancel out, since the wake-field is a function of $t-z/v$, and therefore the integral of T_{xz} in time is independent of z. The remaining terms are given by

$$\int_{-\infty}^{\infty} dt\mathcal{F}_x(t) = -\Delta_y \int_0^{\Delta_z} dz \int_{-\infty}^{\infty} dt T_{xx}(x_{\mathrm{in}},z,t) - \frac{1}{c^2}\Delta_y \int_0^{\Delta_z} dz \int_0^{\infty} dx(\vec{\mathcal{E}} \times \vec{\mathcal{H}}) \cdot \vec{1}_x \Big|_{t=-\infty}^{t=\infty}. \tag{31}$$

The integral of the first term of the above equation over z is trivial since the time integral of T_{xx} is independent of z. In addition, the fields at $t=-\infty$ are zero since the charges have yet to arrive, and the fields at $t=\infty$ are zero as the wake had already escaped from the structure. It follows that the second term of the above equation vanishes as well, and the impulse per unit area reads

$$\Delta p = \frac{1}{\Delta_y \Delta_z}\int_{-\infty}^{\infty} dt\mathcal{F}_x(t) = -\int_{-\infty}^{\infty} dt T_{xx}, \tag{32}$$

where we have omitted the dependence of T_{xx} on time and space. In order to further simplify the impulse integral, we recall that the expression for T_{xx} is given by

$$T_{xx} = \frac{1}{2}\varepsilon_0 \mathcal{E}_x^{\,2} - \frac{1}{2}\varepsilon_0 \mathcal{E}_z^{\,2} - \frac{1}{2}\mu_0 \mathcal{H}_y^{\,2}, \tag{33}$$

where each of the field components is the sum of the primary and secondary contributions. The impulse can be divided into three terms, $\Delta p^{(\mathrm{pri})}$, which is the result of the integration over the square of only the primary fields, $\Delta p^{(\mathrm{sec})}$, resulting from the secondary fields, and $\Delta p^{(\mathrm{pri,sec})}$, which is the result of integration over the cross products, so that

$$\Delta p = \Delta p^{(\mathrm{pri})} + \Delta p^{(\mathrm{sec})} + \Delta p^{(\mathrm{pri,sec})}. \tag{34}$$

Regardless of the velocity of the moving charge v, the first term is identically zero since it corresponds to the case where the charge travels in free space, and therefore $\Delta p^{(\mathrm{pri})}$ represents the impulse experienced by a vacuum region, which is clearly zero. The last term approaches zero as $\gamma\to\infty$, since the primary field is confined to the vicinity of the $\tau=0$ plane, while its intensity is bounded for $x\neq 0$, and consequently, the integral over time vanishes. This can be seen, for example, from the expression of the longitudinal electric primary field, which is given by

$$\mathcal{E}_z^{(\mathrm{pri})} = E_q \frac{\gamma(z-vt)/D_{\mathrm{int}}}{\left[\frac{\gamma(z-vt)}{D_{\mathrm{int}}}\right]^2 + \left(\frac{x}{D_{\mathrm{int}}}\right)^2}. \tag{35}$$

Consequently, only the secondary field is of significance, and recalling that the ultrarelativistic wake is a spectrum of $k_z=\omega/c$ fields, the first and last terms of Eq. (33) cancel out such that $T_{xx}=-\frac{1}{2}\varepsilon_0\mathcal{E}_z^2$, and the impulse integral reduces to

$$\Delta p = \frac{\varepsilon_0}{2}\int_0^{\infty} d\tau(\mathcal{E}_z^{(\mathrm{sec})})^2. \tag{36}$$

This expression for the total impulse is suitable for a single bunch, as well as a finite train of bunches, as will be discussed subsequently.

TABLE I. Comparison between the total wake-field impulse in four structures. Cold and wake-field parameters are also presented. The dominance of the fundamental mode in the impulse is evident.

	Bragg structures		Dielectric loaded TL	
	$D_{\text{int}}=0.3\lambda_0$	$D_{\text{int}}=0.8\lambda_0$	$D_{\text{int}}=0.3\lambda_0$	$D_{\text{int}}=0.8\lambda_0$
Z_{int}/λ_0 [Ω]	400.9	45.0	527.8	50.2
β_{gr}	0.49	0.73	0.64	0.90
α [dB/1000λ_0]	0.13	0.16	0	0
W_{fun}	0.305	0.256	0.759	0.951
Number of modes below $100\omega_0$	977	963	26	13
$\Delta p_{\text{fun}}/(\varepsilon_0 E_Q^2 T_0)$[a]	150.3	105.9	946.9	1486.8
$\Delta p_{\text{nf}}/(\varepsilon_0 E_Q^2 T_0)$[a]	1.1×10^{-3}	1.7×10^{-3}	1.9×10^{-3}	-1.2×10^{-3}
Q [q_e/m][b]	1.7×10^{11}	5.4×10^{11}	6.8×10^{10}	1.4×10^{11}
$\Delta p_{\text{acc}}/(\varepsilon_0 E_Q^2 T_0)$[a]	708.2	282.2	2995.2	2730.4
$\Delta p_{\text{acc}}/(\varepsilon_0 E_0^2 T_0)$[a]	773.7	436.2	526.4	305.8

[a]Values for $L_{\text{acc}}=1000\lambda_0$ and $M=1000$.
[b]Values for $\lambda_0=1.55$ μm.

A simple analytic result may be obtained for the case of a single bunch in a vacuum tunnel bored in a homogeneous dielectric material of permittivity ε_1 [$\mathbb{R}\equiv 0$ in Eq. (19)], for which the secondary field reads

$$\mathcal{E}_z^{(\text{sec})} = E_q \pi e^{-\bar{\tau}} u(\tau). \tag{37}$$

Substituting the above equation into Eq. (36) yields

$$\Delta p = \frac{\pi^2 D_{\text{int}} \sqrt{\varepsilon_1 - 1}}{4\varepsilon_1 c} \varepsilon_0 E_q^2. \tag{38}$$

B. Impulse of a train of microbunches

Efficiency considerations are likely to dictate that a train of microbunches, rather than a single bunch, are to be fed into the optical Bragg acceleration structure. One of the advantages of such an acceleration scheme is that the energy may be recycled, consequently increasing the total efficiency [21]. We, therefore, consider a total amount of charge $-Q$ divided into M microbunches, each of charge $-q$, where $Q=Mq$, separated by a distance λ_0 from each other and traveling at an ultrarelativistic velocity. The wake-field of the train is a superposition of the wake-fields of the individual bunches, and the total resulting field may be substituted into Eq. (36) to obtain the impulse experienced by the structure.

The longitudinal electric field of the train $\mathcal{E}_z^{(\text{sec})}$ can be separated into two terms, one is the contribution of all the bunches to the fundamental mode, and the other is the remainder, namely, the contribution to the nonfundamental modes. The first term represents a buildup of the fundamental mode which adds up in phase, each bunch adding $W_{\text{fun}}\pi E_q$ to the amplitude of the fundamental mode trailing behind it. On the other hand, the nonfundamental modes are not in phase, so that the part of the wake that remains guided inside the structure adds up *incoherently*. It is, therefore, important to distinguish between the two corresponding contributions to the total impulse. We denote by Δp_{fun} the fundamental mode contribution, and the contribution of the nonfundamental, including the cross products between fundamental and nonfundamental modes, is denoted by Δp_{nf}, so that $\Delta p=\Delta p_{\text{fun}}+\Delta p_{\text{nf}}$.

Let us consider the SiO_2-Si Bragg structure described in Sec. IV C, having $D_{\text{int}}=0.3\lambda_0$, and for comparison purposes, we examine three more structures: a similar Bragg structure with $D_{\text{int}}=0.8\lambda_0$, a dielectric loaded metallic transmission line (TL) with $D_{\text{int}}=0.3\lambda_0$, and another with $D_{\text{int}}=0.8\lambda_0$. While the structures having $D_{\text{int}}=0.3\lambda_0$ are single mode, i.e., have only one symmetric TM mode at ω_0, a core half-width of $D_{\text{int}}=0.8\lambda_0$ is large enough so that there are two such modes, which is undesirable. Nevertheless, these structures demonstrate the dependence of the quantities of interest on the core width. The wake-field of the dielectric loaded transmission line, which is treated in Refs. [8,23,24], can be represented in the form of Eq. (27) with $\psi_n\equiv 0$ and $\omega_{1,n}\equiv 0$. The interaction impedance Z_{int}, the normalized group velocity β_{gr}, and the attenuation of the fundamental mode α, which are cold parameters, are presented in Table I for the four structures of interest. The wake-field parameters W_{fun} and the number of wake-field modes below $100\omega_0$ are given as well. It is evident that in the Bragg structure, significantly more modes participate in the wake-field than in the metallic structures, and the fundamental mode is less dominant.

When calculating the contribution of one microbunch to the impulse, we assume that the length of the structure is $L_{\text{acc}}=1000\lambda_0$, and consequently, the wake-field effectively vanishes behind each microbunch after that length, so that the integration of Eq. (36) is carried out up to L_{acc}/c. It is further assumed that above the frequency $100\omega_0$, the materials may be considered transparent ($\varepsilon_r\simeq 1$), and therefore only the modes with $\omega_{\text{R},n}<100\omega_0$ are taken into account. The quantities Δp_{fun} and $|\Delta p_{\text{nf}}|$, as a function of M, are depicted in Fig. 7 for the four structures. All curves are normalized by $\varepsilon_0 E_Q^2 T_0$, where $E_Q \triangleq Q/(2\pi\varepsilon_0 D_{\text{int}})$, and $T_0=2\pi/\omega_0$. For all four structures, $|\Delta p_{\text{nf}}|$ is smaller than 4% of Δp_{fun}, and particularly for the Bragg structures, $|\Delta p_{\text{nf}}|$ is no

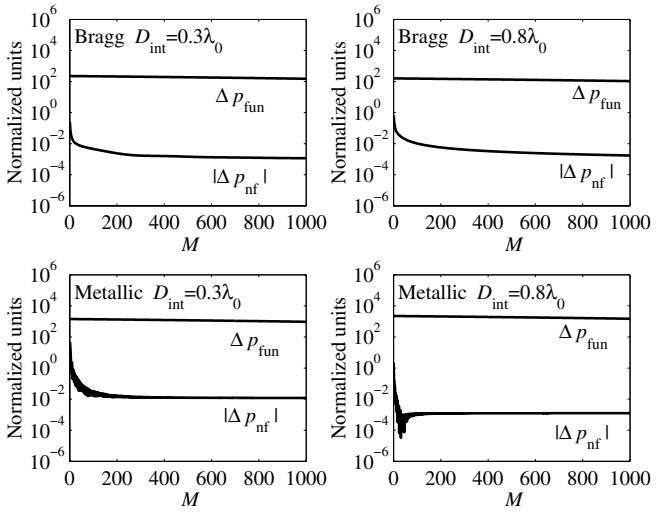

FIG. 7. The fundamental mode contribution to the impulse, Δp_{fun}, and the contribution of the nonfundamental modes, $|\Delta p_{\mathrm{nf}}|$, normalized by $\varepsilon_0 E_Q^2 T_0$, as a function of the number of bunches in the train M, for four structures.

greater than 0.5% of Δp_{fun}. Evidently, the fundamental mode is responsible for almost all of the impact of the wake-field on the structure, and this difference between Δp_{nf} and Δp_{fun} is bigger when W_{fun} is larger, as can be seen in Table I where both values are given for $M=1000$. Note that Δp_{nf} may have negative values, as it includes cross-product terms.

As the impact of the wake-field itself on the guiding structure has been established, we may now give a rough estimate of the impact in a practical acceleration scheme, where both the wake-field and the driving laser are present. Since the length of the moving train is $(M-1)\lambda_0$, and it moves at c, whereas the laser pulse propagates at the group velocity of the structure v_{gr}, it follows that the minimal duration of the laser pulse that ensures overlap of the two is given by

$$\frac{\tau_p}{T_0} = \left(\frac{1}{\beta_{\mathrm{gr}}} - 1\right)\frac{L_{\mathrm{acc}}}{\lambda_0} + \frac{M-1}{\beta_{\mathrm{gr}}}. \tag{39}$$

The laser pulse may be tapered to cancel the decelerating effect of the wake-field on trailing bunches, so that on the average in time, all microbunches are subject to the same accelerating gradient $E_0 \cong 1$ GV/m. Assuming that the laser pulse can peak at $2E_0$, and considering that after the last microbunch, half of this peak cancels the decelerating field, then $MW_{\mathrm{fun}}\pi E_q \approx E_0$. Under this approximation, the total charge that can be accelerated in the train is

$$Q \approx \frac{2\varepsilon_0 D_{\mathrm{int}} E_0}{W_{\mathrm{fun}}}, \tag{40}$$

and the impulse due to both the fundamental mode of the wake and the driving laser is given by

$$\Delta p_{\mathrm{acc}} \approx \frac{1}{4}\varepsilon_0 E_0^2 \tau_{\mathrm{p}} = \frac{1}{4}\varepsilon_0 E_Q^2 W_{\mathrm{fun}}^2 \pi^2 \tau_{\mathrm{p}}. \tag{41}$$

The values of Q for the four structures considered above are given in Table I in terms of the electron charge q_{e} for $\lambda_0=1.55$ μm, as well as Δp_{acc} for $M=1000$. Two normalizations of Δp_{acc} are given in Table I, considering Eq. (41). The first is a normalization by $\varepsilon_0 E_Q^2 T_0$, showing the impulse experienced by the structure relative to the amount of charge accelerated, and therefore, structures with a smaller W_{fun} or a larger v_{gr} (smaller τ_{p}) are favorable. For the $D_{\mathrm{int}}=0.3\lambda_0$ Bragg structure, the total acceleration impulse Δp_{acc} is about five times larger than the wake alone impulse Δp_{fun}, while for the other structures this ratio is smaller.

The second normalization of Δp_{acc} given in Table I is $\Delta p_{\mathrm{acc}}/(\varepsilon_0 E_0^2 T_0)=\frac{1}{4}\tau_{\mathrm{p}}/T_0$, which is relative only to the accelerating gradient, and includes only the influence of v_{gr} through τ_{p}. This normalization allows a comparison between the different structures of the absolute values of the impulse, showing that the largest impulse is of the $D_{\mathrm{int}}=0.3\lambda_0$ Bragg structure, as it has the smaller group velocity. However, the first normalization shows that relative to the amount of charge accelerated, this structure has a smaller impulse than that of the dielectric loaded transmission lines, whose wakes have a large projection on the fundamental mode.

VI. DISCUSSION

Through a detailed analysis of the wake-field in the optical Bragg acceleration structure, it was shown that the impact of the wake on the structure is almost solely due to the fundamental mode. This analysis, which uses the residue theorem in the wake-field integral, emphasizes the distinction between open structures, such as the Bragg structures, and closed structures such as the dielectric loaded planar transmission line. In open structures, moving charges excite a large number of modes, most of which are leaky by nature, exponentially decaying behind the bunch, contrary to closed structures, where truly guided modes are excited. Nevertheless, based on the general proof that was given in Sec. IV B, in both cases the deceleration force on a single particle is identical, depending only on the vacuum tunnel width and the permittivity of the adjacent dielectric layer.

In the $D_{\mathrm{int}}=0.3\lambda_0$ Bragg structure, for instance, the fundamental mode is responsible for only 30% of the deceleration force ($W_{\mathrm{fun}}\approx 0.3$). This may lead to the erroneous conclusion that the remainder of the modes may have a significant impact on the structure. However, the present analysis shows that the nonfundamental modes have a relatively strong exponential decay, or may be guided modes with very small amplitudes. Consequently, the impact that results from the nonfundamental modes is considerably smaller than that of the fundamental, as seen in Fig. 7 and Table I. It is also evident from Table I that the Bragg structure has an advantage over the closed dielectric loaded planar transmission line, since for the same train of bunches, the amplitude of the fundamental mode it excites is lower, thus less interfering with the acceleration of trailing bunches in the train, and creating a smaller impact on the structure.

Since the fundamental mode, which is due partly to the driving laser and partly to the wake-field, is responsible for virtually all of the electromagnetic forces on the structure, it is sufficient to employ the cw analysis of Sec. III in order to examine the possible implications on the acceleration struc-

ture. In addition to the expression for the total transverse pressure given by Eq. (12), we were able to obtain, as an outcome of this analysis, two simple scaling laws for the maximal volume force density [Eq. (16)] and for the maximal surface forces density [Eq. (17)]. We have already stated that the total transverse pressure on one of the Bragg mirrors, as given by Eq. (12), is $\langle F_{x,\mathrm{T}} \rangle \simeq 2.2 \times 10^6$ N/m^2 if we consider an accelerating field of $E_0 = 1$ GV/m. Assuming that one Bragg mirror in the structure has an area of 1×1 mm^2, the total transverse force on the mirror is 2.2 N. For a mirror thickness of 50 μm and material density of about 2 g/cm^3, we obtain that this force is six orders of magnitude larger than the gravitational force on the mirror, indicating that the radiation pressure is by no means negligible.

On the other hand, from the perspective of material strength and the possibility of crack formation, the situation is different. The order of magnitude of the pressures in the $D_{\mathrm{int}} = 0.3\lambda_0$ Bragg structure including the internal pressure $\langle F_{\mathrm{pr}} \rangle$, as shown in Fig. 3, is 10^6–10^7 N/m^2. According to rough theoretical estimates, it would be reasonable to assume that an internal pressure below $E^{(\mathrm{Y})}/\pi$, where $E^{(\mathrm{Y})}$ is Young's modulus, may be sustained without damage to the structure [25]. Young's modulus for SiO_2 is 72.6 GN/m^2, whereas for Si it is 162 GN/m^2 [26]. It follows that the electromagnetic pressures in the structure under consideration are at least three orders of magnitude below the theoretical threshold $E^{(\mathrm{Y})}/\pi$. Moreover, even if D_{int} is increased to $0.8\lambda_0$, there is a difference of more than two orders of magnitude between the obtained pressure and $E^{(\mathrm{Y})}/\pi$. It is also worth noting that a gradient significantly larger than 1 GV/m would be unacceptable since it would cause material breakdown [8] long before reaching the radiation pressure damage threshold. We, therefore, conclude that under the assumptions considered here, the electromagnetic forces on the planar Bragg acceleration structure do not pose a threat to the device.

Finally, we point out that the analysis given here of the effect of a moving electron bunch on the planar Bragg structures may suggest a method of measurement of the amount of charge in the bunch. It may be possible to mechanically measure the instantaneous pressure or total impulse on one of the mirrors, by which estimating the total charge. Such a microsystem may rely, for example, on an *optical spring* where the mirror is balanced from the side opposite to that of the charge by a superposition of two electromagnetic modes [13].

ACKNOWLEDGMENTS

The authors would like to thank Dov Sherman for useful discussions. This study was supported by the Israel Science Foundation and the United States Department of Energy.

[1] Y. C. Huang, D. Zheng, W. M. Tulloch, and R. L. Byer, Appl. Phys. Lett. **68**, 753 (1996).
[2] J. D. Lawson, IEEE Trans. Nucl. Sci. **26**, 4217 (1979).
[3] P. M. Woodward, J. IEE **93**, 1554 (1946).
[4] X. E. Lin, Phys. Rev. ST Accel. Beams **4**, 051301 (2001).
[5] R. P. Larsen and A. A. Oliner, in *IEEE-MTT International Microwave Symposium Digest* (IEEE, Boston, MA, 1967), Vol. 67, pp. 17–22.
[6] P. Yeh and A. Yariv, Opt. Commun. **19**, 427 (1976).
[7] P. Yeh, A. Yariv, and E. Marom, J. Opt. Soc. Am. **68**, 1196 (1978).
[8] A. Mizrahi and L. Schächter, Phys. Rev. E **70**, 016505 (2004).
[9] Z. Zhang, S. G. Tantawi, and R. D. Ruth, Phys. Rev. ST Accel. Beams **8**, 071302 (2005).
[10] A. Mizrahi and L. Schächter, Opt. Express **12**, 3156 (2004).
[11] M. I. Antonoyiannakis and J. B. Pendry, Phys. Rev. B **60**, 2363 (1999).
[12] M. L. Povinelli, M. Ibanescu, S. G. Johnson, and J. D. Joannopoulos, Appl. Phys. Lett. **85**, 1466 (2004).
[13] A. Mizrahi and L. Schächter, Opt. Express **13**, 9804 (2005).
[14] J. Schwinger, J. L. L. DeRadd, K. A. Milton, and W.-Y. Tsai, *Classical Electrodynamics* (Perseus Books, Reading, MA, 1998), p. 39.
[15] M. Planck, *The Theory of Heat Radiation* (Dover Publications, New York, 1959) (translated by M. Masius from the German edition of 1914).
[16] M. Mansuripur, Opt. Express **12**, 5375 (2004).
[17] J. A. Stratton, *Electromagnetic Theory* (McGraw-Hill, New York, 1941).
[18] L. Schächter, R. L. Byer, and R. H. Siemann, Phys. Rev. E **68**, 036502 (2003).
[19] A. V. Oppenheim, A. S. Willsky, and S. H. Nawab, *Signals and Systems*, 2nd ed. (Prentice-Hall, Upper Saddle River, NJ, 1997).
[20] K. L. F. Bane and G. Stupakov, Phys. Rev. ST Accel. Beams **6**, 024401 (2003).
[21] L. Schächter, Phys. Rev. E **70**, 016504 (2004).
[22] F. J. García de Abajo, Phys. Rev. B **70**, 115422 (2004).
[23] A. Tremaine, J. Rosenzweig, and P. Schoessow, Phys. Rev. E **56**, 7204 (1997).
[24] T.-B. Zhang, J. L. Hirshfield, T. C. Marshall, and B. Hafizi, Phys. Rev. E **56**, 4647 (1997).
[25] B. Lawn, *Fracture of Brittle Solids*, 2nd ed. (Cambridge University Press, Cambridge, England, 1995).
[26] M. Bass, E. W. Van Stryland, D. R. Williams, and W. L. Wolfe, *Handbook of Optics Volume II* (McGraw-Hill, New York, 1995).